Journal of The Electrochemical Society, **152** (7) G522-G527 (2005)
0013-4651/2005/152(7)/G522/6/$7.00 © The Electrochemical Society, Inc.

Atomic Layer Deposition of $W_{1.5}N$ Barrier Films for Cu Metallization

Process and Characterization

S. Bystrova,[a,z] A. A. I. Aarnink,[a] J. Holleman,[a] and R. A. M. Wolters[b]

[a]*MESA[†] Research Institute, University of Twente, 7500 AE Enschede, The Netherlands*
[b]*Philips Research Laboratories, Eindhoven, The Netherlands*

An atomic layer deposition process to grow tungsten nitride films was established at 350°C with a pulse sequence of $WF_6/NH_3/C_2H_4/SiH_4/NH_3$. The film composition was determined with Rutherford backscattering as $W_{1.5}N$, being a mixture of WN and W_2N phases. The growth rate was $\sim 1 \times 10^{15}$ W atom/cm^2 per cycle (monolayer of W_2N or WN). The films with a thickness of 16 nm showed root-mean-square roughness as low as 0.43-0.76 nm. The resistivity of the films was stable after 50 cycles at a value of 480 μΩ cm. Results of four-point probe sheet resistance measurements at elevated temperature demonstrated that our films are nonreactive with Cu at least up to 500°C. Results of I-V measurements of p^+/n diodes before and after heat-treatment in (N_2 + 5% H_2) ambient at 400°C for 30 min confirmed excellent diffusion barrier properties of the films.
© 2005 The Electrochemical Society. [DOI: 10.1149/1.1928171] All rights reserved.

Manuscript submitted July 22, 2004; revised manuscript received October 15, 2004. Available electronically May 26, 2005.

Diffusion barrier films are used in back-end interconnects with Cu metallization. The International Technology Roadmap for Semiconductors (ITRS) requires barrier diffusion layers against Cu diffusion scaled down to 7 nm in 2007.[1] Among other requirements, such a thin layer must possess a low roughness and be conformal over features with a high aspect ratio. Advanced ionized physical vapor deposition (iPVD) cannot compete with the excellent step coverage and low roughness of films grown with atomic layer deposition (ALD). The principle of ALD is a repeating, preferably saturated adsorption of reactive species at the surface, resulting in film growth.[2]

Tungsten nitride layers are promising barriers against Cu diffusion.[3,4] Chemical vapor deposition (CVD) of tungsten nitrides using WF_6 and NH_3 is known to suffer from the formation of an adduct WF_6 $4NH_3$ in the cold zones of a reactor.[5] The ALD separates the reactants using a sequential pulsing. This eliminates the formation of this by-product at $T > 325°C$.[6] Klaus *et al.*[7] and Elers *et al.*[8] reported a successful deposition of tungsten nitride with ALD using a repeating cycle with WF_6 and NH_3. Their layers are characterized, however, with a resistivity of 4500 μΩ cm, which is unacceptably high for barrier application. In opposite, the resistivity of ALD- $W_xN_yC_{1-x-y}$ films was reported to be 600-900 μΩ cm for 7 nm films[9] and 350-400 μΩ cm for 25 nm films.[10] $W_xN_yC_{1-x-y}$ layers were grown with a cycling of WF_6,NH_3, and TEB [triethyl borane, $(C_2H_5)_3B$].

We tried ethene, C_2H_4, as a cheap and safe carbon precursor instead of TEB. SiH_4 was used as an extra reducing agent in an additional pulse. However, no carbon was found. The obtained films, as determined with RBS, were tungsten nitrides $W_{1.5}N$, being a mixture of W_2N and WN phases. An established pulse sequence of $WF_6/NH_3/C_2H_4/SiH_4/NH_3$ resulted in layers with a resistivity as low as 480 μΩ cm for films thicker than 13 nm. This resistivity is much lower than the reported values. The obtained films have shown to be excellent Cu barriers. A detailed discussion about pulse sequences and film growth is presented.

Experimental

Deposition equipment.— The ALD system we used is presented schematically in Fig. 1. It consists of a load lock for wafer transfer, an outer chamber, and a small hot-wall reactor inner chamber. The outer chamber (base pressure of 10^{-7} mbar) is purged with N_2 during the process at the same pressure as the operating pressure of the inner chamber. The system is pumped with an oil-free turbopump with a capacity of 400 l/s. This turbopump is backed by a dry pump.

The wafer is placed in the loadlock on a molybdenum susceptor and after pump-down transferred into the chamber by an automated arm and placed on the hot chuck. The chuck goes up and forms the bottom of the hot-wall reactor, creating an enclosed space with a volume of about 24 ml. The upper part consists of the gas block covered with the top heater and a thermo-screen, which protects the outer reactor against heat dissipation. Gas reactants enter the hot-wall reactor via gas distribution channels.

During the deposition a constant flow of 80 sccm N_2 is flowing through the reactor at a total pressure of 1 mbar. The reactant gases were set at 5 sccm via mass flow controllers and are directed into the pump via a bypass system. Sequentially the reactive gases are switched to the reactor chamber during typically 1-3 s where they mix with the N_2. When the precursor gases are switched to the bypass, a nitrogen upstream flow in the precursor line blocks any leaks of the precursor valve and outdiffusion of precursor from dead end parts in the precursor gas line. In between each pulse of reactive gas the reactor is purged with the N_2 for 2 s. This corresponds to a 100-fold purging of the reactor volume. Tests with a 4 s purge did not show any difference. The typical exposure time to reactive gases is 1 s at 1 mbar, which is equivalent to 4.7×10^4 L (langmuir, $1\ L = 10^{-6}$ Torr s). The temperature is regulated by a PID (proportional-integral-derivative) controller via a thermocouple inserted into the top heater. The process temperatures we investigated are 325 and 350°C. Temperatures higher than 400°C are unacceptable for back-end applications. At $T < 325°C$ the incorporation of nitrogen becomes lower.[7]

Deposition process.— *Surface preparation*.— Si(100) n-type 100 mm substrates (1-10 Ω cm) with 700 nm of wet thermally grown SiO_2 were used. Wafers were cleaned in fuming HNO_3 and in boiling 69% HNO_3. Each wafer was dipped in 0.3% HF for 3 min and rinsed in DI water before deposition. This procedure was reported to provide a surface on which dense Si films could grow.[11] The spin-dried wafer was loaded into the reactor.

Nucleation step.—After the process temperature was reached, a Si nucleation film was grown via the decomposition of Si_2H_6 to create reactive sites for the chemisorption of WF_6, similar to Elam *et al.*[12] Without a Si nucleation layer the incubation time was extremely high. The conditions of the nucleation were altered by varying the exposure to Si_2H_6, see Table I. The decomposition was carried out at 10 mbar. The experiments at both temperatures are divided into two groups: with a thick nucleation layer and a thin one. The thick film was made at 4.5×10^9 L at both temperatures. To grow the thin layer with approximately the same thickness at both temperatures, the Si_2H_6 exposures were adapted to 8.1×10^8 L and 2.0×10^9 L at 350 and 325°C, respectively.

[z] E-mail:snbystrova@hotmail.com

Downloaded 29 Jun 2009 to 130.89.112.86. Redistribution subject to ECS license or copyright; see http://www.ecsdl.org/terms_use.jsp

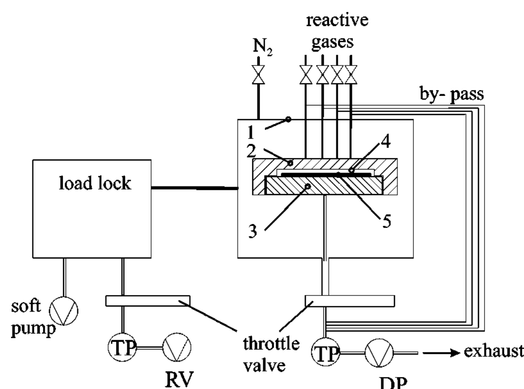

Figure 1. A schematic drawing of the ALD system for barrier deposition: (1) outer chamber, (2) upper part of the hot-wall reactor, (3) hot chuck with susceptor, (4) volume of the hot-wall reactor, and (5) wafer; (TP) turbopump, (RV) rotary-vane pump, and (DP) dry pump.

Film growth.—After the Si-nucleation step the reactor was pumped down from 10 to 1 mbar under Si_2H_6 atmosphere. A cycling sequence of $WF_6/NH_3/C_2H_4/SiH_4/NH_3$ was applied to deposit W_xN_{1-x} films after an N_2-purge pulse. Deposition conditions noted as, *e.g.*, 1/2/3/2/2 refer to the reactant pulse lengths in seconds: 1 s for the WF_6 pulse, 2 s for NH_3, 3 s for C_2H_4, 2 s for SiH_4, and 2 s for NH_3 with pure N_2 purges of 2 s between each reactive gas pulse. The variable parameters were temperature, pulse time, and number of cycles. The cycle time was 14-22 s.

The deposition process was always ended with a SiH_4 pulse in order to obtain a thin layer of Si, meant to protect the barrier against oxidation during unloading the wafer toward atmosphere. The top Si layer was oxidized; thus, a very thin oxide layer of Si is always present on the top of the $W_{1-x}N_x$ films. This was confirmed with XPS measurements.

Compositional and structural analysis.— The composition of the deposited films was measured by X-ray photoelectron spectroscopy (XPS) and Rutherford backscattering spectroscopy (RBS). Occasionally the amount of W was determined from the weight of the deposited layers. XPS profiles were obtained by sputtering with a 1 kV Ar^+ ion beam with an area of 3×3 mm^2. Standard sensitivity factors were used to calculate concentrations. RBS was done with 2 MeV He^+ ions on an area of 1 mm^2. The hydrogen content in the films was determined with elastic recoil detection (ERD). Surface roughness was measured with atomic force microscopy (AFM). X-ray diffraction (XRD) was applied to determine the crystalline structure of the barrier films.

Structures and four-point probe test.— The sheet resistance of the grown barrier films was measured with the four-point probe

Table I. Nucleation conditions.

	T(°C)		Si_2H_6 exposure (L)	Thickness by ellipsometer (nm)	Thickness by XPS (nm)[b]
[a]	350	10 mbar 10 min	4.5×10^9	8-10	
[a]	325	10 mbar 5 min	2.0×10^9	1.2	
[a]	350	10 mbar 2 min	8.1×10^8	1.5	
	350	10 mbar 20 min	8.1×10^9		12
	325	10 mbar 20 min	8.1×10^9		5

[a] Nucleation conditions are used for a detailed study of the process.
[b] Thickness was calculated from sputter time using standard sputter rate.

method. After the $W_{1-x}N_x$ films were deposited, wafers were transferred to the sputtering tool for Cu deposition. The Cu (100 nm)/barrier/SiO_2 (700 nm) stacks on a Si substrate were made for four-point probe *in situ* resistance measurements to study the interaction of Cu with the barrier at elevated temperatures. The measurements were done with a ramp-up and cool-down step of 0.01°/s in vacuum at a base pressure of 4×10^{-6} mbar. After the temperature reached 500°C, it was kept constant for 15 min and then cooled to room temperature.

Diodes were made on (100) n-type Si substrates (1–10 Ω cm). A p^+/n junction was fabricated with BF_2^+ ion implantation at about 0.25 μm depth. Diodes with a varying area between 100 and 1600 μm^2, had a different geometry of the contacts openings and a varying perimeter-to-area ratio. Diodes were tested with barrier thicknesses of 7 and 10 nm. Bare Cu diodes were made with an ultrathin (~3 nm) adhesion layer (Cu reference diodes). I-V measurements of diodes were performed before and after annealing treatment at 400°C in forming gas for 30 min.

Results and Discussion

Growth process.— After a Si nucleation layer has been formed, each growth process starts with a pulse of WF_6. Here the Si nucleation layer reacts with WF_6 as $3Si + 2WF_6 = 2W + 3SiF_4$. The formed W film or nuclei modifies the roughness. For instance, a thick Si nucleation film with a root-mean-square (rms) roughness of 0.25 nm transforms into a W film with a roughness of 1.2 nm. The W nuclei serve as adsorption sites for further deposition. Therefore, in this case, the starting roughness for the growing tungsten nitride film is about 1.2 nm.

Choice of the pulse sequence.— Different sequences of the WF_6, NH_3, C_2H_4, and SiH_4 pulses were studied. The compositions of layers (determined with XPS, RBS), rms roughness, sheet resistance (R), and the layer thickness for different sequences after 100 cycles are presented in Table II.

Table II. Film properties for different pulse sequences after 100 cycles at 350°C.

No.	Nucleation exposure to Si_2H_6 (L)	Pulse sequence	Composition by RBS	Composition by XPS	RMS (nm)[a]	Thickness (nm)[b]	R (Ω/□)
1	4.5×10^9	$WF_6/C_2H_4/NH_3$			1.20	1.4	
2	4.5×10^9	$WF_6/NH_3/C_2H_4$			2.79	5	2970
3	4.5×10^9	$WF_6/NH_3/C_2H_4/SiH_4$	$W_{69.8}N_{30.2}$	$W_{84}N_{16}$	4.19	26	71.3
4	4.5×10^9	$WF_6/NH_3/C_2H_4/SiH_4/NH_3$	$W_{69}N_{31}$	$W_{83}N_{17}$	1.32	26	91.4
5	8.1×10^8	$WF_6/NH_3/C_2H_4/SiH_4/NH_3$	$W_{59}N_{41}$	$W_{80}N_{20}$	0.70	23	170.6
6	4.5×10^9	$WF_6/C_2H_4/SiH_4/NH_3$	$W_{71.4}N_{23.8}Si_{4.8}$	$W_{90}N_5Si_5$	1.76	28	65.5
7	8.1×10^8	$WF_6/NH_3/SiH_4/NH_3$	$W_{49.5}N_{45}Si_{5.5}$	$W_{75}N_{20}Si_5$	0.67	20	178

[a] For a comparison of roughness, the nucleation conditions should be taken into account.
[b] Thickness was calculated using the weight of the film and a standard density of W_2N, 17.8 g/cm^3.

Downloaded 29 Jun 2009 to 130.89.112.86. Redistribution subject to ECS license or copyright; see http://www.ecsdl.org/terms_use.jsp

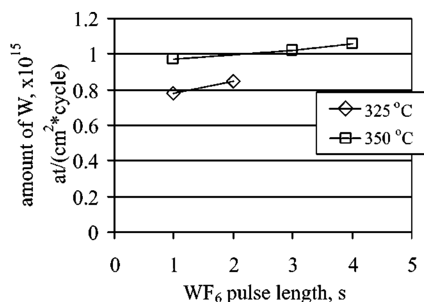

Figure 2. The amount of W deposited per cycle with the WF_6 pulse length. The films were grown at 325 and 350°C.

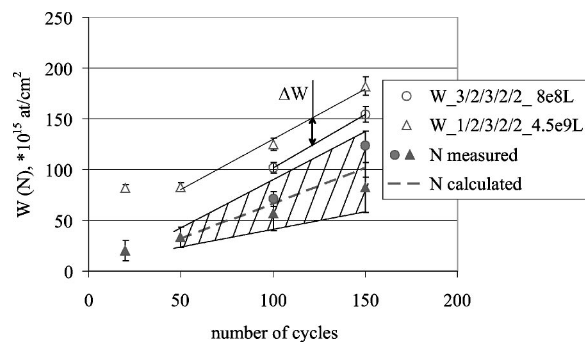

Figure 3. The amount of W and N in the W_xN_{1-x} film *vs.* number of cycles. The film was deposited at 350°C with a sequence of $WF_6/NH_3/C_2H_4/SiH_4/NH_3$. The lengths of reactive pulses and initial exposure to Si_2H_6 are in the legend.

A pulse sequence of $WF_6/C_2H_4/NH_3$ (see no. 1 in Table II) resulted in a roughness of 1.2 nm. This is related to the reaction of WF_6 with Si. No further growth was observed. A plausible explanation for the stopping of the growth is deactivation or poisoning of the W surface with C_2H_4, which decomposes into CH_2 adsorbed on the W surface.[13]

A pulse sequence of $WF_6/NH_3/C_2H_4$ produced a 5 nm film with an rms roughness of 2.79 nm (see no. 2 in Table II). Thus, the layer is hardly continuous. This suggests that only a few reactive sites were available for the reduction of WF_6. To facilitate the formation of new reactive sites an extra SiH_4 pulse was applied.

A sequence of $WF_6/NH_3/C_2H_4/SiH_4$ resulted in a growth of continuous tungsten nitride films (see no. 3 in Table II). No carbon is incorporated in the growing films, despite the C_2H_4 pulse. The Si and F content are at the detection limit of RBS and XPS (<0.5 atom %). The film roughness of 4.2 nm (for 26 nm film) is higher than the roughness of the Si nucleation layer initially (1.2 nm). This roughening is caused by a direct interaction of SiH_{4-x} adsorbed species with WF_6 in the used pulse sequence. Using the sequence of $WF_6/NH_3/C_2H_4/SiH_4/NH_3$, in which the SiH_4 and WF_6 pulses are separated by ammonia, we decreased the roughness to the base value of 1.32 nm (compare no. 3 with 4 in Table II). No change of composition was observed. An even lower rms roughness of 0.7 nm is obtained when we use a thin nucleation layer (see no. 5 in Table II). We found that the thinner the W layer, growing at the cost of Si, the lower the roughness. Thus, the less Si is available to be consumed, the thinner the formed W film is, and the lower its roughness. The resistivity of the layers, calculated as thickness multiplied by sheet resistance, is $\sim 400\ \mu\Omega$ cm (see no. 5 in Table II). For more accurate calculations see the section Film resistance. This value is about ten times lower than reported by Elers *et al.* for their ALD tungsten nitrides grown with WF_6 and NH_3.[8] In their films the amount of the residual F was 2.4 atom%. Thus, the C_2H_4 and SiH_4, introduced in our growth sequence strip off the F during the growth. This might explain why the resistivity of layers is so much lower.

The films deposited with a sequence of $WF_6/(NH_3 = 0)/C_2H_4/SiH_4/NH_3$ contained about 5 atom % Si and had a lower N concentration (see no. 6 in Table II). In the application as a diffusion barrier for Cu metallization Si can diffuse out of the layer into the Cu, causing a rise of resistance. A 0.5 atom % Si in Cu causes a rise of 1 $\mu\Omega$ cm.[14]

Tungsten nitride, deposited with a cycling sequence without ethene $WF_6/NH_3/(C_2H_4 = 0)SiH_4/NH_3$, also contains 5 atom % Si (see no. 7 in Table II).

The explanation for all these differences in composition lies in the reactivity of the W surface terminated by fluorine with the different precursors. The W-F bond is very reactive with both NH_3, SiH_4, and probably, with C_2H_4. When NH_3 is offered as a first step after the WF_6 pulse, many sites are covered with NH_x radicals. The subsequent offering of C_2H_4 and SiH_4 pulses probably do not push the W-NH_x bonds out of their position. The C_2H_4 adsorbing as CH_2 on this surface further occupies sites which are then no longer accessible to SiH_4 chemisorption. So it can be understood that the sequence $WF_6/NH_3/C_2H_4/SiH_4/NH_3$ has the highest N content and lowest Si content. The sequence $WF_6/NH_3/SiH_4/NH_3$ has high amounts of N as well, but also the Si in these films is higher. This is because all sites available to C_2H_4 and SiH_4 in the previous sequence are now available to SiH_4 only. Finally, in the sequence of $WF_6/C_2H_4/SiH_4/NH_3$ most of the available sites are occupied by CH_2 and SiH_x and very few sites are available to NH_3. This results in a lower N content compared to other sequences.

Taking into consideration the composition of the films and the roughness, the sequence of $WF_6/NH_3/C_2H_4/SiH_4/NH_3$ was chosen for further study.

Results of growth study.— A study of the growth rate was done using the RBS data on the amount of W in the films. RBS analysis was performed on the same area and for identical positions for each measured wafer. In this case, the influence of the nonuniformity is minimized.

In Fig. 2 the amount of W deposited per cycle is presented *vs.* WF_6 pulse length. The relative accuracy of the data is 5-10%. The data demonstrate the tendency of increase of the amount of W with a longer WF_6 pulse. At 325°C a double increase of the pulse increases the deposition rate by 7% (see Fig. 2). At 350°C the film growth rate is 15% higher for the same pulse time as compared to 325°C (see Fig. 2). The increase of the WF_6 exposure by three or four times leads to a slight increase of the growth rate by 5-9% (see Fig. 2). We found that per cycle a layer is grown with $\sim 8 \times 10^{14}$ to 1×10^{15} atom/cm^2. This corresponds to about one monolayer of W_2N, which is indicative for an ALD mode of growth. This is comparable to growth per cycle found by Klaus *et al.*,[7] but much more then the growth per cycle found by Elers *et al.*[8]

In Fig. 3 the amount of W and N is plotted *vs.* the number of cycles. These are used for an accurate calculation of the deposition rate at 350°C. The slopes of the W lines are the same for the short and long WF_6 pulse, resulting in a deposition rate of 1×10^{15} W atom/cm^2 per cycle (empty triangles and circles). Therefore this growth process occurs in ALD mode. The difference between the W lines, as well as the deviation of the line from linearity at 20 cycles, is attributed to a difference in the W, which is formed initially very fast at the cost of the Si nucleation layer. The N content is shown as filled shapes in Fig. 3. This determines the film stoichiometry, which is discussed in the following section.

Composition of films.— The composition of layers obtained after 100 cycles with a varying pulse length was determined using XPS and RBS. Both analytical techniques demonstrate that our films are tungsten nitrides.

The accuracy of the amount of nitrogen determined from RBS spectra is between 10 and 30% of the measured value. Consequently, the range of the amount of N in the films becomes very

Downloaded 29 Jun 2009 to 130.89.112.86. Redistribution subject to ECS license or copyright; see http://www.ecsdl.org/terms_use.jsp

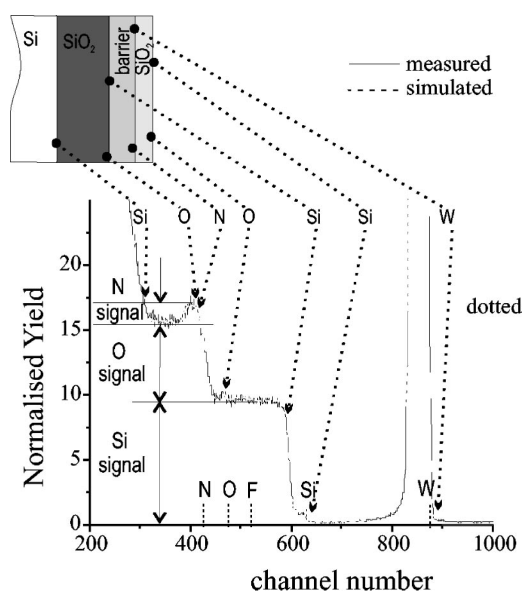

Figure 4. RBS spectrum for a tungsten nitride film grown on 700 nm SiO_2/Si substrate in 150 cycles. The black solid line is the measured signal. The dashed line is the simulation.

broad. This is indicated in Fig. 3 with the shaded area. The inaccuracy comes from the nature of the RBS spectrum. A part of such an RBS spectrum is shown in Fig. 4. A schematic drawing of the measured stack is presented. The dashed arrows demonstrate how the RBS signals are assigned to elements and their location in the depth of the sample. It can be seen that the N signal has the same channel number as the O and/or Si signals from the underlying SiO_2. As a result, the peak from N in the film is on top of Si and O signals. This coincidence of peaks makes an accurate determination of the amount of N very difficult. The error in the calculated amount of N can be as high as 30%. An accuracy of simulated values deteriorates also with less N amount. In this case, a ratio of the N signal to a sum of the Si and O signal degrades and the accuracy becomes worse. The N content in the obtained films was about 38-44 atom% with RBS. The average ratio of W to N content is 1.46 ± 0.13. Given the W growth rate of 1×10^{15} atom/cm^2 (about one monolayer per cycle), the N growth rate is $(0.7 \pm 0.13) \times 10^{15}$ atom/cm^2 per cycle. The calculated N amount in films is indicated in Fig. 3 with the dashed line.

We varied the WF_6 pulse length by a factor of four and the C_2H_4 pulse length by a factor of three, and in other experiments we also varied the sequence and length of other pulses without observing major influences. The fact that no major influences were found with respect to temperature, pulse length, and purge length indicates that we are operating at or close to ALD mode.

An example of an XPS depth profile is presented in Fig. 5. The

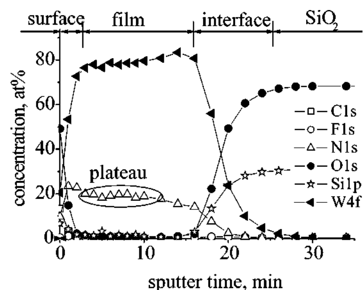

Figure 5. XPS depth profile for a film grown with a pulse sequence of $3/2/3/2/2(WF_6/NH_3/C_2H_4/SiH_4/NH_3)$ at 350°C for 100 cycles.

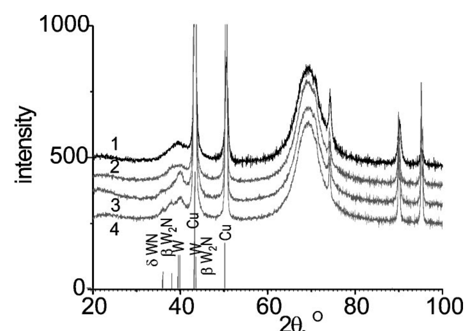

Figure 6. XRD θ-2θ spectrum for the stacks of $Cu/W_{1.5}N$ films.

nitrogen content with XPS was taken from the plateau in the depth profile, where the N and W content did not change anymore. The nitrogen concentration in this case is 15-21 atom %. The depth profile of the samples showed a Si and an O peak at the surface. This corresponds to a very thin intentionally grown Si layer on the top of the ALD film and oxidized later.

The hydrogen content in the films was lower than 1% as measured with ERD.

The average ratio of W to N with XPS is 4.4 ± 0.5. This is substantially higher than the W to N ratio obtained from RBS data. The reason for that is preferential sputtering of nitrogen during depth profiling. This leads to a lower measured value of the N.[15]

Results of XRD analysis.— The results of XRD are presented in Fig. 6. The films have been grown on a thick nucleation layer and covered with a 200 nm Cu film. Cu and Si (from the substrate) show several peaks which could mask peaks in the region $2\theta > 43°$. In the other part of the spectrum all samples show a peak at $2\theta \approx 40°$. This one belongs to β-W or α-W phase formed at the cost of the Si nucleation layer. The peak at $2\theta \approx 36°$ can be assigned to the hexagonal δ-WN phase. The peak at $2\theta \approx 38°$ corresponds to the cubic phases $\beta\text{-}W_2N$ and $\beta\text{-}W_{40.9}N_{9.1}$. The top two curves belong to sequences with longer ethene exposure. They show broader peaks at $2\theta \approx 40°$. Thus, larger exposure to C_2H_4 changes the apparent morphology of the deposited films.

Film roughness.— A film roughness as low as 0.43-0.76 nm was obtained using a low nucleation exposure to Si_2H_6 for 16 nm $W_{1.5}N$ films.

Film resistance.— The sheet resistance (Ω/□) was measured with a four-point probe method. Figure 7 shows the resistance *vs.* the amount of W in the films grown at 350°C using different pulse times. The standard deviation of the resistance is marked with error bars. The resistance is decreasing proportional to the amount of W in

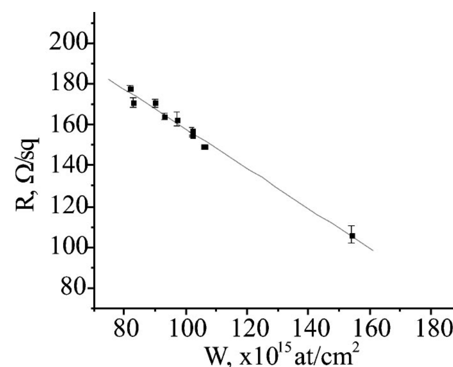

Figure 7. Resistance *vs.* amount of W in films deposited at 350°C using a low nucleation exposure to Si_2H_6.

Downloaded 29 Jun 2009 to 130.89.112.86. Redistribution subject to ECS license or copyright; see http://www.ecsdl.org/terms_use.jsp

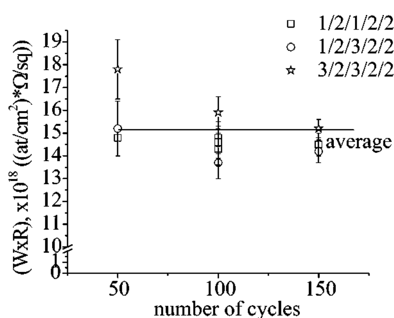

Figure 8. Resistance factor normalized with the amount of W determined with RBS *vs.* number of cycles. The films are grown using a low nucleation exposure to Si_2H_6.

the films. Using the amount of tungsten related to the measured weight increase and multiplied by the measured sheet resistance, a measure for resistivity can be obtained. In Fig. 8 amount of W (W) times the resistance (R), WR, is shown as a function of number of cycles (the film thickness). The factor for resistivity approaches a constant value for films obtained in more than 50 cycles. Obviously, the observed decrease in resistance with the amount of W in Fig. 7 is mainly determined by the thickness of the film itself.

In Fig. 8 the average resistivity value is 15×10^{18} ($\Omega/\square$) (atom/cm^2). Given a measured sheet resistance of 164 $\Omega/\square$, a fifty-fifty distribution of W_2N and WN in the film and their densities from the handbook one can calculate a resistivity of $\sim$480 $\mu\Omega$ cm for our $W_{1.5}N$ films.

Reactivity of Cu and $W_{1.5}N$.— Barrier layers with 100 nm Cu on top were tested by *in situ* four-point probe measurements during heat-treatment. The results (resistance normalized by resistance after heat-treatment) for Cu on SiO_2 and for Cu on $W_{1.5}N$ barriers with a thickness of 17 and 26 nm are presented in Fig. 9a-c, respectively. Upon heating to 250°C, the slope of the curve deviates significantly from the expected linear temperature coefficient of resistance (TCR). A net decrease of resistance is measured after the annealing cycle. At temperatures above 250°C no unexpected change in resistance is observed. The resistivity of the 100 nm Cu layer on oxide (no barrier) was 2.53 and 2.06 $\mu\Omega$ cm before and after anneal at 500°C, respectively. Thus, at low temperatures the resistance of Cu decreases due to the annealing of defects. Table III shows a summary of the test for the 100 nm Cu layer on SiO_2 and the Cu film on the $W_{1.5}N$ layer with a thickness of 17-26 nm. Samples with the 100 nm Cu layer deposited on barriers showed higher sheet resistances than Cu on oxide combination. After annealing, however, the resistivity is close to the value of Cu film on SiO_2. At higher temperatures no reaction between barrier and Cu occurred.

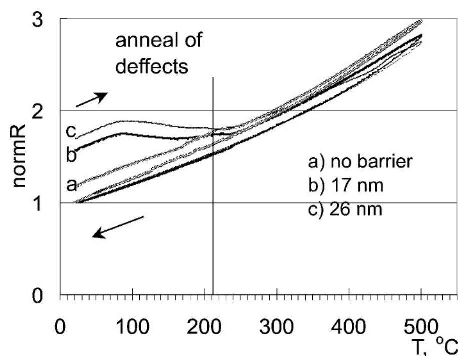

Figure 9. Normalized resistance *vs.* temperature during heat-treatment. Arrows indicate heating and cooling.

Table III. Sheet resistance of Cu layer on barrier films with varying thickness.

No.	Barrier thickness (nm)	R_{before}, (m$\Omega/\square$)	R_{after} (m$\Omega/\square$)
1	no	253	206
2	17	365	235
3	20.5	335	214
4	25.8	450	225
5	26.3	372	220

Some samples were annealed up to 700°C. This high temperature resulted in agglomeration of Cu on the underlying barrier layer. No intermixing of layers was observed and the resistance of the barrier could still be measured. At least up to 500°C no interaction was observed between the barriers and Cu film.

Additionally, diffusion barrier properties of 7 and 10 nm $W_{1.5}N$ films were tested on p^+/n diodes with Cu metallization.[16] Table IV shows the leakage current for diodes before and after heat-treatment at 400°C for 30 min in forming gas. Diodes without a barrier layer demonstrated a huge increase of the leakage current. No increase of leakage attributed to Cu diffusion was observed in diodes with the $W_{1.5}N$ films. Thus, the $W_{1.5}N$ layer is an excellent diffusion barrier against Cu.

The observed decrease of leakage current after heat-treatment for samples 2 and 3 can be attributed to the annealing of interface states.

Conclusions

A repeating pulse sequence of $WF_6/NH_3/C_2H_4/SiH_4/NH_3$ has been shown to grow tungsten nitride films at about one monolayer per cycle at 350°C. The deposited layers are tungsten nitrides with a composition of $\sim W_{1.5}N$ as determined with RBS. No carbon and Si are incorporated. The F content is at the detection limit of RBS and XPS. The resistivity of these layers is $\sim$480 $\mu\Omega$ cm, which is ten times lower than reported before[7,8] for films with 2.4 atom% F deposited without the SiH_4 and C_2H_4 pulse, and this value is at the same level as reported for $W_xN_yC_{1-x-y}$ films.[9,10] Such low resistivity and no F in our films must be either attributed to SiH_4 or C_2H_4 or both gases. When C_2H_4 is set to 0, however, 5 atom % Si is found. Additionally, ethene changes the morphology of the obtained layers. The 16 nm layers are characterized with an rms roughness as low as 0.43 nm.

The diffusion properties were tested on p^+/n diodes with 7 and 10 nm thick $W_{1.5}N$ films. No leakage current increase attributed to a Cu diffusion and/or barrier failure was measured after a heat-treatment at 400°C for 30 min in forming gas. Thus, the $W_{1.5}N$ layers have excellent barrier properties against Cu diffusion. The interaction between Cu and $W_{1.5}N$ are tested with the four-point probe *in situ* resistance test at elevated temperatures. $W_{1.5}N$ layers of 17 nm thickness stayed nonreactive with Cu at least up to 500°C anneal under vacuum conditions. The combination of the low rms roughness, low resistivity, temperature stability of the $Cu/W_{1.5}N$ combination, and diffusion properties demonstrate that these films are good diffusion barriers.

Table IV. Leakage current for diodes with the area of $(1600\ \mu m)^2$ before and after heat-treatment.

No.	Barrier thickness (nm)	$I_{leakage\ before}$ (pA)	$I_{leakage\ after}$ (pA)
1	0	37	59000
2	7	11	1.7
3	10	72	3.1

Downloaded 29 Jun 2009 to 130.89.112.86. Redistribution subject to ECS license or copyright; see http://www.ecsdl.org/terms_use.jsp

Acknowledgments

Authors are grateful to Yde Tamminga, Hans Hendriks, and Hans Snijders from Philips Research for film analysis and valuable discussions of the results. We gratefully thank Suvi Haukka from ASM Microchemistry for her advice. This project was financially supported by Philips Semiconductors.

The University of Twente assisted in meeting the publication costs of this article.

References

1. *International Technology Roadmap for Semiconductors (ITSR)* (2003).
2. T. Suntola, *Mater. Sci. Rep.*, **4**, 261 (1989).
3. T. Nakajiama, K. Watanabe, and N. Watanabe, *J. Electrochem. Soc.*, **134**, 3175 (1987).
4. C. Ahrens, G. Friese, R. Ferretti, B. Schwierzi, and W. Hasse, *Microelectron. Eng.*, **33**, 301 (1997).
5. K.-M. Chang, T.-H. Yeh, I-C. Deng, and C.-W. Shih, *J. Appl. Phys.*, **82**, 1469 (1997).
6. J. W. Klaus, S. J. Ferro, and S. M. George, *Appl. Surf. Sci.*, **162-163**, 479 (2000).
7. J. W. Klaus, S. J. Ferro, and S. M. George, *J. Electrochem. Soc.*, **147**, 1175 (2000).
8. K.-E. Elers, V. Saanila, P. J. Soininen, W.-M. Li, J. T. Kostamo, S. Haukka, J. Juhanoja, and W. F. A. Besling, *Chem. Vap. Deposition*, **8**(4), 149 (2002).
9. S. Smith, W.-M. Li, K.-E. Elers, and K. Pfeifer, *Microelectron. Eng.*, **64**, 247 (2002).
10. W.-M. Li, K. Elers, J. Kostamo, S. Kaipio, H. Huotari, M. Soininen, P. J. Soininen, M. Tuominen, S. Haukka, S. Smith, and W. Besling, *IEEE 2002, International Interconnects and Technology Conference* (2002).
11. K. Nakagawa, M. Fukuda, S. Miyazaki, and M. Hirose, *Mater. Res. Soc. Symp. Proc.*, **452**, 243 (1997).
12. J. W. Elam, C. E. Nelson, R. K. Grubbs, and S. M. George, *Thin Solid Films*, **386**, 471 (2001).
13. G. Robertshaw and P. J. Estrup, *J. Vac. Sci. Technol.*, **15**(2), 554 (1978).
14. S. Bystrova, J. Holleman, P. H. Woerlee, and R. A. M. Wolters, in *SAFE Proceedings*, Veldhoven, The Netherlands (2000).
15. J. L. Alay, H. Bender, G. Brijs, A. Demesmaeker, and W. Vandervorst, *Surf. Interface Anal.*, **17**, 373 (1991).
16. S. Bystrova, J. Holleman, A. A. I. Aarnink, and R. A. M. Wolters, *Mater. Res. Soc. Symp. Proc.*, To be published.

Downloaded 29 Jun 2009 to 130.89.112.86. Redistribution subject to ECS license or copyright; see http://www.ecsdl.org/terms_use.jsp